PHYSICAL REVIEW B VOLUME 36, NUMBER 17 15 DECEMBER 1987-I

Electronic properties and superconductivity of rapidly quenched Al-Si alloys

J. Chevrier,* D. Pavuna,† and F. Cyrot-Lackmann
Laboratoire d'Etudes des Propriétés Electroniques des Solides, Centre National de la Recherche Scientifique,
Boîte Postale No. 156X, 38042 Grenoble Cédex, France

(Received 24 July 1987)

We present detailed studies of electronic properties of Al-Si alloys prepared in a nonequilibrium state by means of rapid solidification. The quenched alloys exhibit an enhanced superconducting transition temperature up to 6.2 K in an Al–Si 30 at. % alloy as well as an increased thermal slope of resistivity. Using differential scanning calorimetry, a large enthalpy variation ($\Delta H = 4.1$ kJ/mole for Al–Si 30 at. %) has been measured during the irreversible transition from the nonequilibrium state to the equilibrium one. This is mainly attributed to the energy difference between the metallic state of silicon atoms trapped in fcc aluminum matrix during quenching and the usual covalent state of silicon precipitates in an equilibrium state. This large energy difference is presented as the origin of a lattice instability which softens the phonon spectrum and gives rise to a stronger electron-phonon coupling. This appears to be a characteristic property of nonequilibrium Al-Si solid solutions, which is associated with the metallic state of silicon atoms. An interpretation of the T_c enhancement is proposed for both Al-Si and Al-Ge alloys based on the phonon softening in these nonequilibrium crystalline alloys.

I. INTRODUCTION

When prepared in a nonequilibrium state by either rapid solidification,[1] evaporation,[2] or ion implantation,[3] the aluminum-rich Al-Si alloys exhibit striking electronic properties such as an enhanced T_c as compared with pure aluminum. On the other hand, at the equilibrium, the electronic properties are very close to those of pure aluminum due to the fact that silicon and aluminum are nearly immiscible elements. Therefore it is important to know what structural changes occur which can be a cause of a T_c enhancement of about 5 K. As a possible interpretation, a new kind of electron coupling[4,5,1] was proposed based on the existence of a great number of disordered metal-semiconductor interfaces. To our knowledge, no experimental evidence of this mechanism has been given in the case of rapidly quenched Al-Si alloys. In any case, this gives rise to the fact that one has to consider the coexistence of two elements as different as a metal and a semiconductor to analyze the electronic properties of nonequilibrium Al-Si alloys. However, a semiconductor state is not the only possible state of silicon, two metallic states also exist: the liquid state with a disordered structure and different crystalline states under high pressure characterized by a coordination number always higher than 4 like in the covalent structure.[6] Moreover, as the superconducting transition temperature T_c is an important property of the Al-Si alloys nonequilibrium state, we note that experimental studies have demonstrated that silicon (and in general semiconductors) becomes superconducting under high pressure with T_c close to the values found in our alloys.[7] Furthermore, to explain the occurrence of rather high T_c in these pure simple metals obtained under high pressure, theoretical analysis has also raised the point that close to a metal-semiconductor transition,[8] a lattice instability can occur which could lead to an enhancement of electron-phonon coupling due to associated soft phonon modes. Recently, this has been experimentally studied in pure silicon.[9,10]

In this context we have investigated the properties of rapidly quenched Al-Si alloys in order to find out the structural modification which could lead two elements usually well separated to interact so strongly that important new electronic properties can arise. We present a detailed structural analysis based on x-ray diffraction and electron microscopy. As the nonequilibrium state seems to be an important condition to observe these effects, we have used differential scanning calorimetry (DSC) to analyze the enthalpy difference between the nonequilibrium and the equilibrium state. High-temperature scanning resistivity gives a direct correlation of the thermal structural variation and the transport properties evolution during annealing. The study of electronic properties has been achieved by means of resistivity measurements as temperature was varied between 1.5 and 200 K and low-temperature specific-heat measurements. This last technique was used to check that the superconducting state was a bulk one while the resistivity was used to measure both T_c and the thermal resistivity slope, which are important means to investigate any electron-phonon-coupling variation. All the new experimental features found in the quenched alloys appear to be due to the silicon atoms trapped in the fcc aluminum matrix in a metallic state. We present an interpretation which emphasizes the energy difference between the covalent and the metallic states of silicon as the main cause of the enthalpy difference between the nonequilibrium and the equilibrium states and a Debye temperature decrease as the origin of the electron-phonon-coupling enhancement. We compare calculated T_c within the framework of MacMillan theory and experimental values for Al-Si and Al-Ge alloys. Our main experimental conclusion is that usually semiconductor elements that remain metallic by quenching in a metallic matrix can induce a nonequilibrium state with new electronic properties.

II. EXPERIMENT

A. Sample preparation and characterization

$Al_{1-x}Si_x$ alloys have been prepared with silicon concentration varied as follows: $x=0$, 1.65, 3, 6, 12, 20, and 30 at. % Si. Master alloys were prepared by induction melting in an argon atmosphere. We homogeneized the master ingots by repeating the melting procedure several times. The aluminum ingots were 99.99% quality and those of silicon 99.999%. The rapidly quenched ribbons were produced using a multimode melt spinning apparatus described in a previous publication.[11] Helium atmosphere was used to improve thermal exchange and to limit oxidation. The roller speed was 40 m/s, and as estimated from the ribbon thickness (about 30 μm), the magnitude of the cooling rate was 10^6 K/s. With a possible length of few meters, the ribbon width was about 2 mm. As far as possible, for all the samples prepared, the quenching parameters were kept constant. The microstructure of the quenched alloys was analyzed by means of x-ray diffraction with a goniometer using the copper $K\alpha$ wavelength. In order to obtain the distribution, the chemical composition and the characteristic length of each phase, a scanning transmission electron microscopy (STEM) analysis was performed. The microstructural analysis has already been the subject of a publication; therefore, only the main results are summarized here.

The usual equilibrium phase diagram structures were found in all the rapidly quenched samples investigated by x-ray diffraction (Fig. 1). However, two important differences were noticeable. (i) The lattice parameter of the fcc aluminum phase has always been found to be smaller than 4.049 Å, the pure aluminum value. In an Al–20 at. % Si alloy, the lattice was 4.035 Å. As shown by Itagaki *et al.*,[12] this is an indication of a strain induced by a silicon supersaturation of the aluminum matrix. This decrease appears to be a specific character of the quenched alloy as the covalent silicon atomic volume (20 Å^3) much larger than the aluminum one (16.6 Å^3) prevents any kind of simple extrapolation to analyze the experimental variation of the lattice parameter (in fact, the atomic volume found in metallic silicon, 15.5 Å^3 for β-Sn structure, is much closer to aluminum). (ii) The peaks of the covalent silicon phase also found on the diffraction pattern were very broad and from a simple profile lines analysis; we have estimated the grain size to be about 10 nm. Despite this relatively simple x-ray diffraction pattern, STEM analysis has been necessary to obtain the actual phase repartition. Generally, in the samples analyzed an homogeneous aluminum-rich phase was found with an average grain size of several hundred nanometers, but varying in an Al–20 at. % Si from 10 nm on the wheel side of the ribbons to 1 mm on the free side. In this sample, local chemical analysis by STEM revealed an average supersaturation of about 8% of silicon. Using the lattice parameter variation with silicon concentration found for alloys with an amount of silicon smaller than the solubility limit,[13] the same supersaturation has been deduced from the lattice parameter variation. However, the cross-section analysis shows that this is only an average, the silicon concentration decreasing when coming from the wheel side down to the free side. This can be seen as a cooling-rate variation across the ribbons due to the fact that the most efficient thermal exchange are limited to the wheel side. The same analysis for Al–6 at. % Si and Al–2 at. % Si alloys has indicated a supersaturation of about 4% for the first and between 5% and 6% for the last. Between regions of aluminum-rich phase, covalent silicon-rich grains have been found with their usual diamond structure. The typical size estimated on the photograph was close to the 10 nm deduced from x-ray-line broadening. In some Al–20 at. % Si samples, diffuse diffraction rings existed, corresponding to interplane distances of 3.2 and 1.9 Å. This appears to be evidence for a covalent silicon amorphous phase.

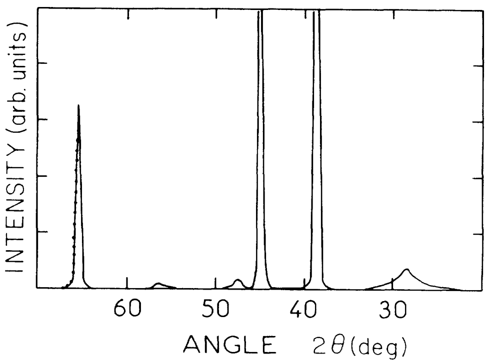

FIG. 1. X-ray diffraction pattern obtained on an Al–20 at. % Si in the quenched state.

Therefore rapidly quenched Al-Si alloys of different compositions have been found to contain two very different phases. The most important is a large fcc aluminum-rich phase supersaturated with silicon atoms. Its characteristic length is about 100 nm. Due to the silicon atoms trapped in during crystallization, its lattice parameter is decreased. The second, generally in between the grains of the previous one, is a covalent silicon-rich phase formed generally by small diamond grains and in some samples by an amorphous phase.

B. Measurements

The irreversible transition between the nonequilibrium state and the equilibrium state has been investigated by means of a differential scanning calorimetry, DSC2 Perkin Elmer. This measurement enabled us to investigate the enthalpy difference between the nonequilibrium and the equilibrium states. The use of three different heating rates (10, 20, and 40 K/min) gave us the activation energy involved in the return to equilibrium using a Kissinger-type procedure.[14] High-temperature resistivity has been measured using the standard four-probe technique. The oven was equipped with an automatic temperature control based on a chromel-alumel thermocouple and filled with a slight overpressure of helium gas. A heating rate of 5 K/min was achieved with a good temperature control. The contacts were made with gold wires embedded in a gold glue. The heating rate used during DSC and resistivity measurements were closed enough to compare the kinetics obtained in both cases. The low-temperature measurements were performed in a helium flux cryostat in the temperature range 1.5–300 K. The temperature was measured by a calibrated Fe-Rh resistance in the whole range. The computerized temperature control provided a stability close to 0.01 K. The resistivity measurements were made using a 1–10 mA dc current and four pressure contacts. Due to the uncertainty in the geometrical factor, the experimental error on resistivity is about 10%. The specific heat was measured in an apparatus based on the flux-flow method described in detail in Ref. 15. The temperature range of specific-heat measurements was 1.5–4.2 K.

III. RESULTS

A. Irreversible transition between nonequilibrium and equilibrium states

DSC measurements on rapidly quenched Al-Si alloys display at about 450 K a large exothermal effect. This effect exists for all the silicon concentrations investigated (between 6% and 30%). At the same temperature an important irreversible decrease of the resistivity is found which is an evidence for the influence of the new microscopic structure on the electronic properties of these rapidly quenched alloys. In Figs. 2 and 3 we show the DSC spectrum and the resistivity difference between the quenched and the annealed states for two very different silicon concentrations (6% and 20%). From DSC measurements, we deduce two experimental values: (i) the activation energy E_a deduced from the variation of the exothermal peak highest point using different heating rates; (ii) the enthalpy difference ΔH between the quenched state and the annealed state. These results are presented in Table I. The activation energy, which seems to be a constant for all the concentrations investigated, is close to the characteristic value for silicon diffusion in an aluminum matrix $E_a = 110$ kJ/mole.[16] This is a strong indication that this exothermal effect is mainly due to the silicon atoms rejected out of the aluminum matrix by thermally activated diffusion. Moreover, an estimate of the temperature transformation can be made if we use the data for silicon diffusion in aluminum.[16] Table II contains the thermal diffusion length of a silicon atom during 1 min, which is a characteristic time of our measurements. As compared to the structural dimensions, the thermally activated diffusion becomes important at about 450 K, which is roughly the temperature of the irreversible variation of the resistivity. Therefore the rejection out of the aluminum matrix of silicon atoms trapped during rapid solidification appears to be the main cause of the irreversible decrease of the resistivity and of the large simultaneously observed exothermal effect. The enthalpy variation associated with this transformation is about 30–40 kJ for each silicon mole in solution as estimated from the aforementioned silicon concentrations in aluminum.

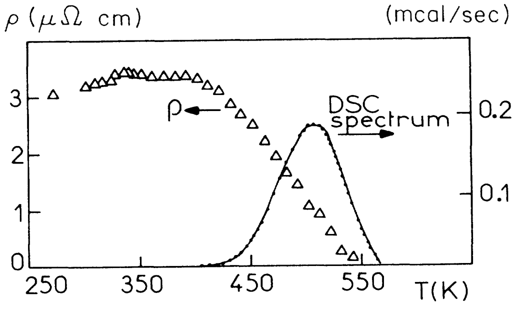

FIG. 2. DSC spectrum (·) and irreversible resistivity variation (△) for an Al–6 at.% Si alloy (DSC heating rate 10 K/min).

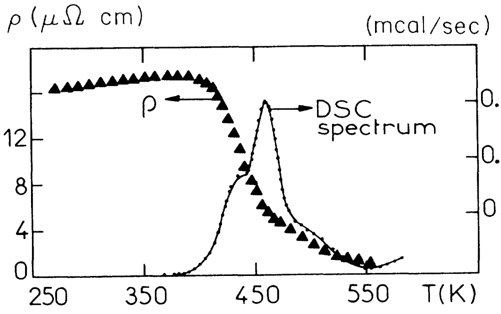

FIG. 3. DSC spectrum (·) and irreversible resistivity variation (▲) for an Al–20 at.% Si alloy (DSC heating rate 10 K/min).

In order to specify the influence of the irreversible transformation on the electronic properties, the variation of T_c after annealing has been measured. In Fig. 4 the decrease of T_c of an Al–30 at.% Si alloy is shown. The temperatures of the annealing are close to the characteristic temperature observed in the previous thermal experiments, and the two different curves are obtained, respectively, for 363 K (90 °C) and 373 K (100 °C). This behavior appears as an indication that again the silicon thermally activated diffusion controls the decrease of T_c.

TABLE I. Enthalpy variation and activation energy for different silicon concentrations deduced from DSC measurements.

x (at.% Si)	ΔH (kJ/mole)	E_f (kJ/mole)
6	0.9	110
12	2.2	110–120
20	3.7	100
30	4.1	100

TABLE II. Diffusion length of silicon in aluminum after 1 min at different temperatures.

d (Å)	T (K)
0.3	320
5	370
30	420
200	470
700	520

This is strongly supported by the fact that the solid-solution lattice parameter exhibits the same kinetic behavior when the sample is annealed.[12] Therefore our conclusion is that the trapping of silicon atoms in the aluminum matrix during rapid solidification is the main structural change which could explain the resulting electronic properties of these nonequilibrium alloys.

B. Low-temperature properties of rapidly quenched alloys

In the preceding section, we have seen how the superconducting transition temperature is affected by annealing. In this section we analyze how the electronic properties of the rapidly quenched Al-Si alloys are with varying the silicon concentration. The superconducting transition temperatures for different silicon concentrations are shown in Fig. 5. They have been determined by resistivity measurements. The enhancement has been observed in all the compositions: in the highest Al–30 at. % Si as in the lowest Al–3 at. % Si. However, all the superconducting transition are rather broad, especially at high silicon concentrations (about 1 K at 30 at. % Si). As discussed in the preceding section, the quenched alloys are fairly inhomogeneous and the variation of the structural properties across the ribbon section could be one of the reasons for the broadening of T_c. To complete the analysis of the superconducting transition, specific-heat measurements have been performed on ribbons of different concentrations (see Fig. 6). The characteristic jump at the superconducting transition can be seen for all the samples, but is still very broad. The T_c enhancement is confirmed for all the silicon concentrations investigated and the values here obtained are close to these obtained by resistivity measurements. This is a clear indication that most of the metallic phase is superconducting and a rough estimate of the ratio $\Delta C/\gamma T_c$ gives a value close to 1.4. Hence the superconducting state is of bulk type even if the inhomogeneities in the samples give rise to a broadening of superconducting transitions. As the bulk metallic phase is involved in the superconducting state, the enhancement of T_c is clearly due to the structural change of the fcc-rich aluminum phase.

In Table III residual resistivities measured just above T_c for very different silicon concentrations are presented. In these inhomogeneous materials, whatever the composition, the residual resistivity is always smaller than 15 $\mu\Omega$ cm, which is typical of a metallic behavior. Moreover, the electronic mean free path can be estimated using the relation $\rho l = 400$ $\mu\Omega$ cm Å, deduced from Ref. 17. It is always smaller than the typical aluminum grain size. Thus the electrical conduction is determined by the electronic properties in the fcc-rich aluminum phase. The temperature dependence of the resistivity is essen-

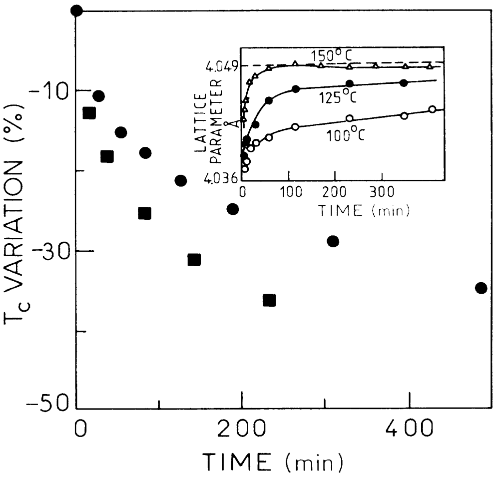

FIG. 4. Superconducting transition temperature variation of an Al–30 at. % Si alloy after isothermal annealing (●, $T=363$ K; ■, $T=373$ K). In inset, lattice parameter variation after isothermal annealing is presented from Ref. 12.

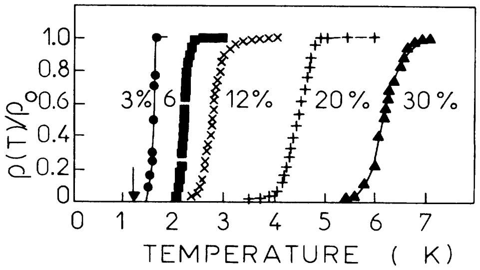

FIG. 5. T_c measured by resistivity on as-quenched Al-Si alloys (●, Al–3 at. % Si; ■, Al–6 at. % Si; ×, Al–12 at. % Si; +, Al–20 at. % Si; ▲, Al–30 at. % Si).

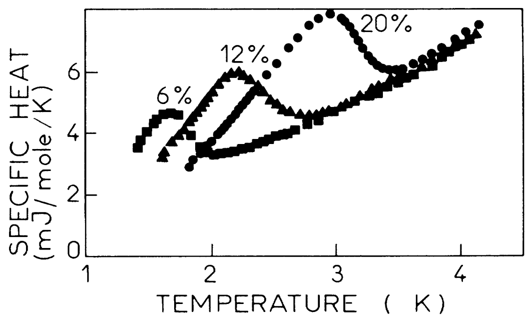

FIG. 6. T_c measured by means of specific-heat measurements on as-quenched Al-Si alloys (■, Al–6 at. % Si; ▲, Al–12 at. % Si; ●, Al–20 at. % Si).

TABLE III. Residual resistivity for different silicon concentrations.

ρ_0 ($\mu\Omega$ cm)	x (at. % Si)
1	1.6
1.5	3
2.5	6
7	12
12	20
(15)	30

tially due to the properties of the aluminum-rich phase. In Fig. 7 the temperature dependence of the resistivity is shown for different silicon concentrations. They are typical curves observed in a metallic regime with a linear part at high temperature as could be expected from the low-residual-resistivity values. We note that the thermal part of resistivity is constantly enhanced as the silicon concentration is changed from 6% up to 20%. Moreover, in order to show that this is a direct consequence of quenching, we present in Fig. 8 the thermal resistivity for an Al–20 at. % Si in the quenched state and after complete annealing at a temperature higher than 450 K. As the electrical resistivity is determined by the metallic phase only, this is experimental evidence for an electron-phonon-coupling enhancement in the rich fcc aluminum phase which is consistent with an enhancement of the superconducting transition temperature. As the only structural change in aluminum matrix induced by quenching is the large increase of the silicon solubility, the conclusion arises that the enhancement of both T_c and the slope resistivity are mainly due to the silicon atoms in the fcc aluminum matrix. In order to go a step beyond, we have analyzed the thermal variation of resistivity using the Bloch-Grüneisen theory[17] with the $J_5(x)$ Debye function in order to determine if the electron-phonon-coupling variation could be attributed to a phonon spectrum change in these nonequilibrium crystalline materials (i.e., we have taken into account the deviation from the Matthiessen law due to the stronger electron-phonon coupling). This calculation enables us to estimate the Debye temperature from the shape of the resistivity curve, and the results are represented by solid lines in Fig. 8. The Debye temperature found for the annealed sample ($\Theta_D = 370$ K) is close to the data ($\Theta_D = 390$ K) published for pure aluminum.[18] As at equilibrium the thermal resistivity is expected to be determined only by the nearly pure aluminum phase, this result is not surprising. For the as-quenched alloy, the agreement between the calculated curve and the measured values is as good as it was for the annealed state. But the estimated Debye temperature is found to be much smaller than in the equilibrium alloy ($\Theta_D = 280$ K). This suggests that the difference in the electron-phonon-coupling enhancement in the nonequilibrium state as compared to the equilibrium, is mainly due to the softening of the phonon spectrum. As previous results indicated that all the change in the electronic properties were due to the trapping of silicon atoms in the fcc aluminum matrix, this softening appears correlated with the occurrence of a supersaturated silicon aluminum solid solution.

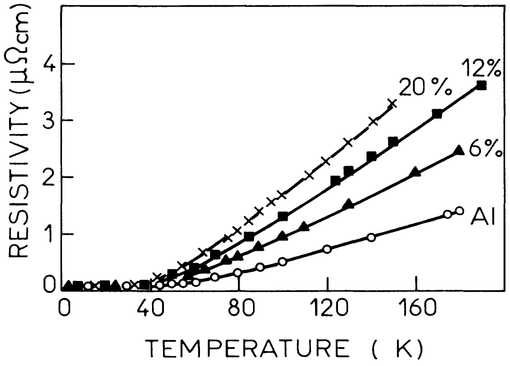

FIG. 7. Thermal variation of the resistivity for different silicon concentrations (○, Al; ▲, Al–6 at. % Si; ■, Al–12 at. % Si; ×, Al–20 at. % Si). For each alloy the residual resistivity has been subtracted.

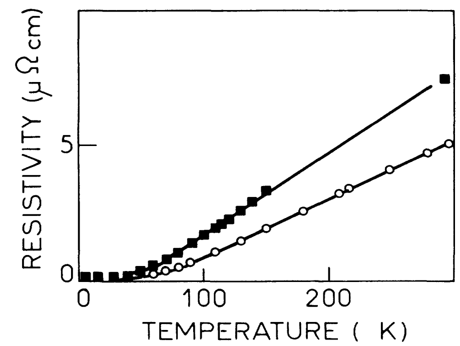

FIG. 8. Difference of thermal resistivity in the as-quenched state and in the annealed state for an Al–20 at. % Si (■, as-quenched state; ○, annealed state). The solid lines are the calculated curves to obtain the Debye temperature.

IV. DISCUSSION

On the basis of the aforementioned experimental results on rapidly quenched Al-Si alloys, we conclude that less than 10% of silicon dissolved in an fcc aluminum matrix gives rise to an exothermal effect as large as about 4 kJ/mole, a T_c enhancement of several kelvin and a large Debye temperature decrease. As deduced from the high-temperature measurements, the exothermal effect is due to the rejection of the silicon out of the aluminum matrix in the silicon covalent precipitates. Thus the corresponding enthalpy difference which is between 30 and 40 kJ per each silicon mole rejected appears to be the energy difference between a metallic state of silicon atoms with 12 first neighbors in aluminum and the usual covalent state with four neighbors in the silicon phase. This energy can roughly be evaluated from the anomalous latent heat of fusion of silicon: the silicon liquid state is metallic and the solid-liquid transition also include a semiconductor-metal transition. Analysis of this point by different authors[19,20] gave an energy ΔE_f between 35 and 40 kJ/mole which is very close to our estimate. Therefore this metallic state of silicon imposed by the fcc symmetry of the aluminum, is in our interpretation, the major cause of the nonequilibrium state in these rapidly quenched alloys. As the enthalpy difference between quenched and annealed states is strongly increasing with the dissolved silicon concentration, the question arises of how do the properties of the fcc lattice change. The characteristic energy associated with the occurrence of a rigid lattice is the latent heat of fusion L_f. The aluminum latent heat of fusion being $L_f(\mathrm{Al})=10.7$ kJ/mole,[21] ΔE_f is therefore much larger than $L_f(\mathrm{Al})$. This suggests that a lattice instability could occur in this nonequilibrium crystalline state and could be described by

$$L^* = L_f(\mathrm{Al}) - x^* \Delta E_f \ , \tag{1}$$

where x^* is the silicon concentration in aluminum. Moreover, the latent heat of fusion can be correlated to the Debye temperature using an extended Lindemann formula:[22]

$$\Theta_D = C(L_f/M)^{1/2} \ , \tag{2}$$

where C is fairly constant for pure metals. Relation (2) can be derived from the Lindemann formula using the fact that the entropy of fusion is nearly a constant for pure metals. This enables us to link the structural properties of solid state which determine L_f to the dynamical properties as described in the low-frequency regime by the Debye temperature. In the case of aluminum silicon solid solution, no latent heat of fusion can be determined as this alloy is not in an equilibrium state, but the energy associated with the appearance of the fcc lattice is L^*.

Empirically it is possible to use L^* in relation (2), which gives the following relation (3) to be compared with experimental results:

$$\Theta_D \mathrm{Al}_{1-x^*}\mathrm{Si}_{x^*} = \Theta_D(\mathrm{Al})[1 - x^* \Delta E_f(\mathrm{Al})]^{1/2} \ . \tag{3}$$

C has been considered as the same for both pure aluminum and Al-Si solid solution and then eliminated. For Al–20 at.% Si, the Θ_D calculated is 300 K using $\Theta_D = 370$ K for an annealed alloys as shown on Fig. 7 and experimental data $\Delta H = 3.7$ kJ/mole as $x^* \Delta E_f$. Compared with the value estimated from experimental result, $\Theta_D = 280$ K, the calculated value is of the same order of magnitude. Thus using this simple model, it is possible to show that about 8% of silicon dissolved in aluminum can be sufficient to decrease Θ_D by as much as 20%. Within the framework of MacMillan analysis,[23] the superconducting transition temperature can be calculated in order to see whether this reduced Debye temperature can account for the enhancement in T_c measured in quenched samples. As the crystallographic structure of the rich-aluminum phase always has the fcc symmetry and as, within a simple electronic model, the perturbation of the metallic silicon on the electronic structure of the metallic phase is small in this range of concentration, the Hopfield parameter, $\eta = N(E_F)\langle I^2 \rangle$, and the Coulomb interaction parameter can be considered constant for all the silicon concentrations investigated. Therefore we use usual values for these parameters, normally used for pure aluminum.[23] With the rough assumption that the electron-phonon-coupling parameter λ can be determined by using the Debye temperature instead of $\langle \omega^2 \rangle$, T_c can be directly calculated from the following relations:[23]

$$T_c = \frac{\Theta_D}{1.45} \exp\left[-1.04 \frac{(1+\lambda)}{\lambda - \mu(1+0.62\lambda)} \right] , \tag{4}$$

$$\lambda = \lambda_0 / (1 - x^* \Delta E_f / L_f) \ , \tag{5}$$

where $\mu = 0.1$ and $\lambda_0 = 0.38$. In Fig. 9, the superconducting transition temperatures deduced from relations (4) and (5) are compared with our experimental values together with T_c measured on samples prepared under high pressure,[24] which extends to higher silicon concentrations the comparison with this model. We note that in Ref. 24 results are also presented for Al-Ge alloys which exhibit similar behavior but with a slightly smaller T_c maximum. The same analysis can be done for this alloy but with a smaller value for $\Delta E_f = 25$ kJ/mole (taken out of Ref. 19). This difference on ΔE_f between silicon and germanium is presumably due to their difference on metallicity as shown in Ref. 25.

As can be seen from Fig. 9, there is a good agreement between experimental data and calculated values. The difference in T_c maximum between germanium and silicon at high semiconductor element concentration is also well described by our model. Within our interpretation, this means that the phonon softening induced by the metallic state of the semiconductor element is large enough to explain the T_c enhancement experimentally observed.

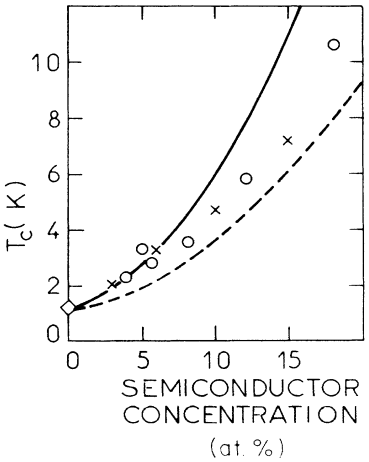

FIG. 9. Experimental T_c for AlSi and AlGe alloys compared to calculated curves (see text). AlSi experimental data: ○, our samples and results of Ref. 24. AlGe experimental data: ×, Ref. 24. The solid line is the calculated curve for AlSi alloys and the dashed line is for AlGe alloys.

V. CONCLUSION

Our study of the rapidly quenched Al-Si alloys shows that they are very different from the as-cast alloys. In fact, because there is no mutual solubility and no compounds, electronic properties of aluminum-rich alloys at equilibrium, like the superconducting transition temperature, are very close to those of pure aluminum. Rapid quenching of Al-Si alloys increases the superconducting transition temperature, residual resistivity, and the thermal slope of the resistivity, but these metastable alloy remain metallic and the fcc crystallographic structure of aluminum is not changed. The calorimetry studies reveal a large enthalpy difference between the as-quenched and the annealed states. The irreversible behavior of the resistivity is associated with this energy variation at 450 K and links the electronic properties to the structural transformation. All these effects are experimentally correlated. Thus they have been simultaneously found in all the compositions investigated. The analysis of all experimental results indicates that the silicon atoms trapped in the aluminum matrix during rapid quenching are the main cause of T_c, $d\rho/dT$, and ρ_0 enhancements and of the nonequilibrium state of these alloys. We analyze the variation of $d\rho/dT$ as due to a marked softening of the phonon spectrum which is large enough to account for the large enhancement of T_c. The enthalpy difference ΔH between the two states can be seen as the difference between the metallic state of the silicon atoms in the fcc aluminum matrix and the covalent state in silicon grains. We have developed an interpretation to link the nonequilibrium state induced by metallic silicon atoms to the dynamical properties in the long-wavelength limit. This enables us to describe the influence of a silicon concentration less than 10% on the properties of rapidly quenched Al-Si alloys such as a T_c enhancement or a Debye temperature decrease.

ACKNOWLEDGMENTS

We would like to thank P. Germi (Laboratoire de Cristallographie, Centre National de la Recherche Scientifique, Grenoble, France) for x-ray measurements, P. Sainfort (Centre de Recherche et Développement de Pechiney, Voreppe, France) for STEM analysis, D. Moody (University of Leeds, U. K.) for specific-heat measurements, R. Perrier de la Bathie (Laboratoire Louis Néel, Centre National de la Recherche Scientifique, Grenoble, France) for help in master ingots synthesis. This work has been supported by Agence Française pour la Maitrise de l'Energie.

---

[*] Present address: Institut Max von Laue–Paul Langevin, Boîte Postale No. 156X, 38042 Grenoble Cédex, France.

[†] Present address: Institut de Physique Appliquée, Ecole Polytechnique Fédérale de Lausanne, CH-1015 Lausanne, Switzerland.

[1] C. C. Tsuei and W. L. Johnson, Phys. Rev. B **9**, 4742 (1974).

[2] F. Meunier, J. J. Hauser, H. P. Burger, E. Guyon, and M. Hesse, Phys. Lett. **28B**, 37 (1968).

[3] A. M. Lamoise, J. Chaumont, F. Lalu, F. Meunier, and H. Bernas, J. Phys. Lett. **37**, 287 (1976).

[4] D. Allender, J. Bray, and J. Bardeen, Phys. Rev. B **7**, 1020 (1973).

[5] V. L. Ginzburg, Usp. Fiz. Nauk **101**, 185 (1970) [Sov. Phys.—Usp. **13**, 335 (1970)].

[6] J. P. Gaspard, Ph. Lambin, C. Mouttet, and J. P. Vigneron, Philos. Mag. B **50**, 103 (1984).

[7] J. Wittig, Z. Phys. **195**, 215 (1966); K. J. Chang, M. M. Dacorogna, M. L. Cohen, J. M. Mignot, G. Chouteau, and G. Martinez, Phys. Rev. Lett. **54**, 2375 (1985).

[8] K. J. Chang and M. L. Cohen, Phys. Rev. B **30**, 5376 (1984); M. L. Cohen and P. W. Anderson, in *Superconductivity in d- and f-Band Metals,* Proceedings of the Conference on Superconductivity in *d*- and *f*-band Metals, edited by D. H. Douglass, AIP Conf. Proc. No. 4 (AIP, New York, 1972), p. 17.

[9] J. M. Mignot, G. Chouteau, and G. Martinez, Phys. Rev. B **34**, 3150 (1986).

[10] S. Minomura, in *High Pressure and Low Temperature Physics,* edited by C. W. Chu and J. A. Wollam (Plenum, New York, 1977).

[11] J. Chevrier, P. Sainfort, P. Germi, and D. Pavuna, in Proceedings of the 3rd Conference on Noncrystalline Materials, Grenoble, 1985, edited by C. Janot and A. F. Wright [J. Phys. (Paris) Colloq. **12**, C8-533 (1985)]. J. Chevrier, Ph. D. thesis, University of Grenoble, France, 1985.

[12] M. Itagaki, B. Giessen, and N. J. Grant, Trans. Am. Soc. Met. **61**, 330 (1968).

[13] S. C. Agarwall, M. J. Koczak, and H. Herman, Scr. Metall. **7**, 365 (1973).

[14] H. E. Kissinger, Anal. Chem. **29**, 1702 (1957).

[15] T. Ng, Ph. D. thesis, Leeds University, United Kingdom, 1984.

[16] C. Smithells, *Metals Reference Book,* 3rd ed. (Butterworths, London, 1962).

[17] G. Grimvall, in *Selected Topics in Solid State Physics,* edited by E. P. Wohlfarth (North-Holland, Amsterdam, 1981), Vol. 16, p. 14.

[18] *American Institute of Physics Handbook,* 2nd ed. (McGraw-Hill, New York, 1963).

[19] B. K. Chakraverty, J. Phys. Chem. Solids **30**, 454 (1969).

[20] J. A. Van Vechten, Phys. Rev. B **7**, 1479 (1973).

[21] B. Chalmers, *Principles of Solidification* (Wiley, New York, 1967).

[22] F. Lindemann, Z. Phys. **11**, 609 (1910).

[23] W. L. MacMillan, Phys. Rev. B **167**, 331 (1968).

[24] V. F. Degtyareva, G. V. Chipenko, I. T. Belash, O. I. Barbalov, and E. G. Ponyatovskii, Phys. Status Solidi A **89**, K127 (1985).

[25] W. A. Harrison, *Electronic Structure and Properties of Solids (Physics of Chemical Bond)* (Freeman, San Francisco, 1980), p. 88.